



1 **A high-accuracy dynamic dilution method for generating reference gas**
2 **mixtures of carbonyl sulfide at sub-nanomole-per-mole levels for long-term**
3 **atmospheric observation**

4

5 Hideki Nara, Takuya Saito, Taku Umezawa, Yasunori Tohjima

6

7 National Institute for Environmental Studies, 16-2 Onogawa, Tsukuba, Ibaraki 305-8506, Japan

8

9 *Correspondence to:* Hideki Nara (nara.hideki@nies.go.jp)

10



1 **Abstract.** Atmospheric carbonyl sulfide (COS) has received increasing attention as a potential tracer
2 for investigating the global carbon cycle. Owing to the irreversible photosynthetic absorption of COS,
3 changes in the atmospheric COS mole fraction can be related to terrestrial gross primary production.
4 However, the instability of COS in high-pressure cylinders has hampered the accurate determination of
5 atmospheric COS. Here, we report a dynamic dilution method for generating reference gas mixtures
6 containing COS at ambient levels (ca. 500 pmol mol⁻¹). Our method combined a dynamic dilution
7 system employing a high-accuracy mass flow measurement system and a gravimetrically prepared
8 parent gas mixture containing a micromole-per-mole level of COS filled in a high-pressure aluminium
9 cylinder, the COS stability of which we experimentally validated for at least 10 years. We evaluated the
10 dilution performance of the developed method using a gravimetric parent gas mixture containing
11 approximately 1 μmol mol⁻¹ of COS and chlorodifluoromethane (HCFC-22). In our evaluation
12 experiments, excellent repeatability (0.23% for COS and 0.43% for HCFC-22 in terms of relative
13 standard deviation), reproducibility (COS: 0.04%, HCFC-22: 0.28%), and dilution linearity ($R^2 > 0.99$,
14 for both COS and HCFC-22) were obtained. The dilution accuracy was examined by comparing the
15 determined HCFC-22 mole fractions in a dynamically diluted parent gas mixture from a mass flow rate
16 measurement system and gas chromatography–mass spectrometry (GC/MS) calibrated using a
17 gravimetrically diluted parent gas mixture. The mole fractions of HCFC-22 from these two methods
18 agreed within an acceptable difference of approximately 2 pmol mol⁻¹, validating the dilution accuracy
19 of the developed method. By re-evaluating the experimental data, we determined the mole fractions of
20 COS and HCFC-22 in an ambient air-based reference gas mixture, with relative standard errors of 0.02%
21 for COS and 0.12% for HCFC-22. These results demonstrated that the developed method can accurately
22 generate reference gas mixtures containing COS at ambient levels, which we expect will support long-
23 term observations of atmospheric COS.

24

25



1 **1. Introduction**

2 Carbonyl sulfide (COS) is the most abundant sulphur-containing compound in the atmosphere. It acts
3 as a sulphur carrier from the troposphere to the stratosphere, contributing to the distribution of
4 stratospheric sulphate aerosols that influence Earth's radiative balance (Chin and Davis, 1995;
5 Kjellstrom, 1998; Brühl et al., 2012). Atmospheric COS has recently received increasing attention as a
6 potential tracer for examining the global terrestrial carbon cycle (Montzka et al., 2007). Unlike CO₂,
7 COS is irreversibly taken up by terrestrial plants on via photosynthesis (Goldan et al., 1988; Protoschill-
8 Krebs et al., 1996; Sandoval-Soto et al., 2005; Seibt et al., 2010; Stimler et al., 2010, 2012), allowing
9 the estimation of terrestrial gross primary production from the local to the global scale based on
10 atmospheric COS observations (Campbell et al., 2008; Blonquist Jr et al., 2011; Asaf et al., 2013;
11 Commane et al., 2013; Maseyk et al., 2014; Wehr et al., 2016; Yang et al., 2018; Kooijmans et al., 2019).
12 For example, the inter-annual variability in the global annual mean mole fraction of atmospheric COS
13 has been used to estimate the biogeochemical feedback of terrestrial plant ecosystems in response to an
14 increase in atmospheric CO₂ levels (Campbell et al., 2017). The World Meteorological Organization has
15 estimated the inter-annual variability of COS to be only several picomoles per mole in the global
16 background atmosphere over the last two decades (WMO, 2018), highlighting the need for technical
17 methods that allow precise determination of atmospheric COS levels.

18 Despite promising new directions for estimating global terrestrial gross primary production using
19 COS, atmospheric COS observations are insufficient for understanding its global distribution and budget.
20 The fundamental reason for this is the difficulty in establishing reliable reference gas mixtures
21 containing ambient levels of COS (ca. 500 pmol mol⁻¹) due to the poor stability of COS stored in high-
22 pressure cylinders (Hall et al., 2014). Indeed, as demonstrated in this study (see Figure 3 in Section 3),
23 the changes in the mole fraction of COS in the cylinder during storage (hereafter referred to as COS
24 drift) can be greater than the inter-annual variability of COS. To better understand spatial and temporal
25 variations in atmospheric COS, observations on a stable calibration scale that is compatible across
26 multiple laboratories are required. Thus, approaches to addressing issues related to the storage instability
27 of COS are required.



1 Gravimetric preparation, in which individual gas components are weighed into a cylinder, is the
2 most common approach for producing reference gas mixtures containing long-lived trace gases such as
3 CO₂, CH₄, and N₂O (ISO, 2015). Although this approach is the most accurate, it is time-consuming and
4 generally requires multistep dilutions when preparing a gas mixture at the sub-nanomole-per-mole level.
5 This multistep procedure results in the accumulation of preparation uncertainty. In addition, the prepared
6 gas mixtures were filled in a gas cylinder, in which storage stability was not guaranteed for gases such
7 as COS.

8 Dynamic dilution is an alternative approach to gravimetric preparation (ISO, 2018). Historically,
9 various dynamic dilution methods have been applied to gas species that exhibit strong adsorption or
10 limited stability at ambient levels in high-pressure cylinders (Goldan et al., 1986; Fried et al., 1990;
11 Wright et al., 1994; Kerwin et al., 1996; Mohamad et al., 1996; Nakao et al., 1999; Goody et al., 2002;
12 Brewer et al., 2011, 2014; Flores et al., 2012; Kim et al., 2016; Guillevic et al., 2018; Macé et al., 2022).
13 A major advantage of dynamic dilution is that the reference gas mixture can be generated from a pristine
14 parent gas mixture immediately before analysis, which eliminates the need for storage and therefore,
15 prevents any possible mole fraction change that could occur over time. However, only a few studies
16 have used dynamic dilution to generate diluted gas mixtures at the sub-nanomole-per-mole level with
17 high accuracy (Kim et al., 2016; Guillevic et al., 2018). Moreover, the application of this method is
18 limited to gas species with a clear stability at high mole fractions in high-pressure cylinders. To the best
19 of our knowledge, there have been no reports on dynamic dilution-based techniques for generating sub-
20 nanomole-per-mole reference gas mixtures of COS.

21 Here, we report a dynamic dilution method for the preparation of reference gas mixtures containing
22 COS at ambient levels, which we expect will support long-term atmospheric COS observations. In
23 Section 2, we present a detailed description of the dynamic dilution system developed in this study,
24 estimate the theoretical dilution uncertainty, and describe the procedure for determining the mole
25 fraction of COS in a generated gas mixture. In Section 3, we examine the long-term stability of COS
26 stored in a high-pressure aluminium cylinder. In Section 4, we evaluate the dilution performance and
27 overall dilution accuracy of our method and provide an example of the mole fraction assignment for



1 COS in an ambient air-based reference gas mixture. In Section 5, we discuss the possible causes of
2 dilution bias observed for COS in this study. All experiments were designed based on a series of
3 preliminary studies (hereafter referred to as our pilot study), which are detailed in the Supplementary
4 Information.

5

6 **2. Materials and methods**

7 Figure 1 shows the schematic of our dynamic dilution system. Briefly, the system generates the desired
8 gas mixture by blending two gas flows of a gravimetrically prepared parent gas mixture containing a
9 few micromole-per-mole fractions of COS and a COS-free diluent gas. Dilution accuracy is achieved
10 by a high-accuracy flow measurement system that has been used as a dynamic dilution method to
11 generate sub-micromole-per-mole reference gas mixtures and adjust the composition of gas matrices
12 (Brewer et al., 2014; Nara et al., 2012). A detailed description of the main components of the dilution
13 system is provided in Section 2.1; a general explanation of the generation of a dynamically diluted gas
14 mixture is provided in Section 2.2; a theoretical estimation of the dilution uncertainty is discussed in
15 Section 2.3; and the determination of the COS mole fraction in a dynamically generated gas mixture
16 combined with a gas chromatography–mass spectrometry (GC/MS)-based sample determination system
17 is provided in Section 2.4.

18

19 **2.1 Main components of the dilution system**

20 The dilution system consisted of two gas cylinders, a high-accuracy flow measurement system, four
21 mass flow controllers (MFCs), a static mixer, and an automatic back-pressure regulator (ABPR). These
22 components are described in detail below.

23

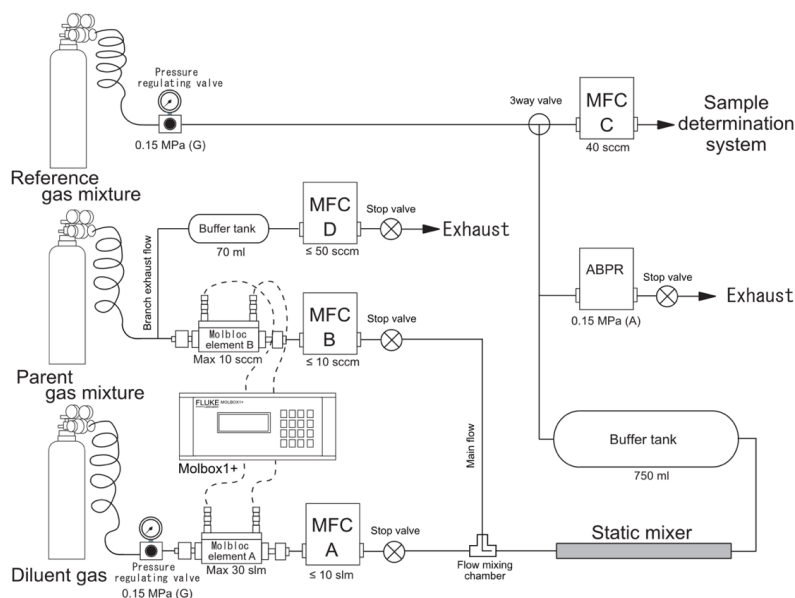
24 **2.1.1 Parent and diluent gases**

25 A gas mixture of COS and chlorodifluoromethane (HCFC-22) was used as the parent gas with a high-
26 purity nitrogen balance. The parent gas mixture was prepared gravimetrically by a Japanese gas
27 manufacturer (Japan Fine Products Co., Kanagawa, Japan) and was provided in a 9.4-L high-pressure



1 aluminium cylinder at a fill pressure of 9.81 MPa (unless otherwise noted, gas pressures are reported on
2 the gauge scale). The inner surface of the cylinder was polished using a proprietary method to reduce
3 adsorption of COS and HCFC-22. The nominal mole fractions of COS and HCFC-22 were 1.01 and
4 $1.00 \mu\text{mol mol}^{-1}$, respectively. HCFC-22 was added to the parent gas mixture to aid in assessing the
5 presence and extent of the dilution bias (see details in Supplementary Information). HCFC-22 was
6 selected because (1) its atmospheric dry mole fraction is relatively close to that of COS (approximately
7 $260 \text{ pmol mol}^{-1}$ in northern hemispheric background air; cf. COS: $400\text{--}600 \text{ pmol mol}^{-1}$) (WMO, 2022)
8 and (2) it is more stable than COS with respect to adsorption. High-purity nitrogen (>99.99995% purity;
9 Japan Fine Products, Co.) filled in a 47-L high-pressure manganese steel cylinder was used as the diluent.
10 The outflow pressures from the parent and diluent gas cylinders were regulated using single-stage
11 (AEROTRACE; Nissan Tanaka Corp., Saitama, Japan) and two-stage stainless steel pressure regulators
12 (SuperLabo; Nissan Tanaka Corp.), respectively.

13 The presence of COS as a contaminant in the diluent gas was verified before each experiment using
14 a sample determination system (see Section 2.4). Three different COS-free gases filled in high-pressure
15 cylinders were examined: purified air (Japan Fine Products, Co.), in which H_2O and atmospheric trace
16 gases were removed by cryogenic separation (Nara et al., 2012); high-purity nitrogen (>99.99995%
17 purity; Japan Fine Products, Co.); and high-purity helium (>99.99995% purity; Japan Fine Products,
18 Co.). Nitrogen and helium were used as the diluent gas in our dilution system and as the carrier gas for
19 the sample determination system, respectively. Small amounts of COS (but not HCFC-22) were detected
20 in all the three gases. However, the COS signals were comparable, suggesting that the contamination
21 was likely due to the constant blank of COS in the determination system. This blank check ensured that
22 there was no COS contamination from the diluent or carrier gases, which may have biased the
23 determination of COS and HCFC-22 in our experiment.



1

2 **Figure 1: Schematic of the dynamic dilution system. The thermal-based mass flow controllers and**
3 **automatic back-pressure regulator are denoted as MFC and ABPR, respectively. Full-scale**
4 **volume flow rates (FS) that determine the flow precision are provided for each Molbloc element**
5 **and thermal-based mass flow controller.**

6

7 **2.1.2 High-precision flow measurement system**

8 A Molbloc high-precision flow measurement system (Fluke Co., WA) was used to measure the mass
9 flow rates of the diluent and parent gases. The system comprised a system controller (Molbox 1+) and
10 two Molbloc-L laminar mass flow elements (A, model 3E4 VCR-V-Q and B, model 1E1 VCR-V-Q).
11 The full-scale volume flow rates of the diluent and parent gases were 30 standard liters per minute (slm)
12 and 10 standard cubic centimetres per minute (sccm), respectively. The Molbloc system accurately
13 calculates the mass flow rate based on measurements of the temperature and the upstream and
14 downstream pressures of the gas flow passing through the element in a laminar regime according to the
15 Hagen–Poiseuille law (Landau and Lifshitz, 1987). System control and data acquisition were performed
16 using the Tera Term software (version 4.97; Tera Term, 2017). The maximum measurement uncertainty



1 depended on the flow rate and was $\pm 0.2\%$ of the measured value or $\pm 0.02\%$ of the full-scale flow rate
2 at flow rates above and below 10% of the full-scale flow rate.

3

4 **2.1.3 Thermal-based MFCs**

5 Our dynamic dilution system used four thermal-based MFCs (A–D). MFC-A and -B (SEC-Z712MGX;
6 HORIBA STEC, Co., Ltd., Kyoto, Japan) were used for automatic flow control of the diluent and parent
7 gases, respectively, with full-scale flow rates of 10 slm and 10 sccm, respectively. MFC-C was the same
8 model as the controller but with a full-scale flow rate of 300 sccm and was used to control the outflow
9 of the dynamically generated gas mixture from the dilution system. The flow precision of these three
10 MFCs was $\pm 1.0\%$ of the set point or $\pm 0.25\%$ of the full-scale flow rate for above and below 25% of
11 their full-scale flow rate, respectively. The inner surfaces of the MFCs were mirror polished to prevent
12 gas adsorption. The fourth controller, MFC-D (SEC-400MK3; HORIBA STEC, Co., Ltd.), was used to
13 control the exhaust of the excess parent gas for dynamic buffering of the parent flow pressure with a
14 precision of 2% for a full-scale flow rate of 100 sccm, with a limited operating range of over 5% of the
15 full-scale flow rate. Each MFC was operated individually using a control unit (PD-D20; HORIBA STEC,
16 Co., Ltd.).

17

18 **2.1.4 Static mixer**

19 A static mixer (G 1/4-18; Noritake, Co., Ltd., Aichi, Japan) was used to facilitate blending of the diluent
20 and parent gas flows. The gas mixer was a 1/4-inch internal diameter SUS316 stainless steel pipe with
21 a length of 215 mm. The mixing fin assembly consisted of 18 elements and was set within the pipe. The
22 inner surface of the pipe and outer surfaces of the mixing fin assembly were electrically polished to
23 prevent gas adsorption.

24

25 **2.1.5 ABPR**

26 An ABPR (UR-Z722M-UC-B; HORIBA STEC, Co., Ltd.) was used to exhaust the excess diluted gas
27 mixture from the system and ensure that the pressure within the system remained constant. The ABPR



1 operated at an absolute operating pressure range of 10–300 kPa and controlled the pressure with a
2 precision of 0.5% for the full-scale operating pressure (corresponding to ± 1500 Pa), resulting in the
3 pressure inside the system being independent of the barometric variations. The ABPR was controlled
4 using the same unit as that used to control the MFCs. The gas contact area along the entire flow path
5 was an all-metal construction with a mirror polished surface.

6

7 **2.2 General description of the dynamic dilution system**

8 Our dynamic dilution system is similar to that developed by Brewer et al. (2014) but was modified by
9 installing a branch exhaust system to accurately generate gas mixtures containing sub-nanomolar-per-
10 mole levels of COS.

11 When starting the system, we purged it for at least 15 min with the parent and diluent gases supplied
12 from the high-pressure cylinders at the flow rates set in the subsequent dilution experiment. Before each
13 gas dilution, conditioning purge was performed for 15 min (only first gas dilution needed 30 min purge
14 at least). During this 15-min purge, the flow pressures of the two gas flows were adjusted to match each
15 other within ± 0.3 kPa based on the pressure readings from the Molbloc elements. Although the mass
16 flow rates of the two gas flows were controlled by MFC-A and -B, using these MFCs alone resulted in
17 insufficient pressure matching between the two flows. Therefore, for more precise pressure control,
18 additional pressure stabilisation techniques were used for each gas flow because their mass flow rates
19 were substantially different; for example, the flow rate of the diluent gas was 2000-times larger than
20 that of the parent gas when generating a diluted gas mixture containing COS at ambient levels of
21 approximately $500 \text{ pmol mol}^{-1}$.

22 The flow pressure of the diluent gas was controlled using a cylindrical regulator and simple in-line
23 pressure regulator (6600A; Kofloc Corp., Kyoto, Japan). The flow pressure of the diluent gas was first
24 set at 0.24 MPa using the cylinder regulator and was further adjusted using the in-line pressure regulator
25 set at 0.15 MPa to suppress the pressure change in response to regulator cooling owing to adiabatic
26 expansion of the outflowing gas. In contrast, the parent gas was introduced into the flow-mixing
27 chamber along the main flow path at a flow rate usually limited to 10 sccm, with the outflow pressure



1 set by the cylinder regulator at 0.15 MPa. At such a low flow rate, the instability of the cylinder regulator
2 becomes pronounced, leading to pressure fluctuations of several thousand pascals. Because this pressure
3 fluctuation is difficult to remove by passing through a MFC, we installed a branch exhaust system
4 located upstream of the flow-measuring element in the Molbloc system. The system exhausted the parent
5 gas along the branch exhaust flow path via a 70-mL glass buffer tank at a flow rate of more than 10
6 sccm, which was higher than the flow rate of the main flow. This branch exhaust system prevented the
7 dilution biases found in our pilot study (see Supplemental Information: the dilution biases are discussed
8 in detail in Section 5) and dynamically buffered any pressure changes to facilitate the stabilisation of
9 the parent flow pressure, which should match that of the diluent gas during gas dilution. The diluent and
10 parent gas flows were controlled by MFC-A and -B, which were placed in the respective flow paths
11 downstream of the Molbloc elements and converged in a flow-mixing chamber. The flow-mixing
12 chamber was made of a 1/4-inch outer diameter stainless steel T-fitting, in which one port was connected
13 to a bored-through reducer. The diluent gas flowed straight from upstream to downstream, while the
14 parent gas tube (1/16-inch outer diameter) was inserted from the side port of the T-fitting through the
15 reducer and was bent at a right angle in the downstream direction so that the parent gas flow was
16 introduced into the diluent gas flow in the flow direction. After the convergence of the two flows in the
17 chamber, the generated gas mixture was passed through the static mixer to complete gas blending and
18 then into a glass tank (volume: 750 mL) to buffer any pressure changes in the blended gas mixture.

19 Finally, the diluted gas mixture was supplied to the sample determination system via the MFC-C.
20 Excess flow was exhausted through the ABPR set at an absolute backpressure of 0.15 MPa, which
21 prevented the influence of barometric changes outside the system. The expected mole fractions of COS
22 and HCFC-22 in the generated gas mixture were accurately calculated from the mass flow rates
23 measured using the Molbloc system. To prevent the possible loss of COS by adsorption, a Sulfinert
24 coating (Restek Corporation, PA) was applied to all tubes, fittings, and valves that were exposed to the
25 parent gas and generated gas mixtures.

26

27 **2.3 Estimation of uncertainty for the gas dilution**



1 The mole fraction of gas x in a dynamically generated gas mixture can be calculated using the mole
2 fraction of the target gas in the gravimetric parent gas mixture, mass flow rates of the parent and diluent
3 gases under the assumption of complete mixing of the two gases, and constant mole fraction of gas x in
4 the gas flow from the parent gas cylinder. The mole fraction of gas x is expressed as follows:

$$6 \quad [x]_{diluted} = \frac{[x]_{parent} \cdot f_{parent}}{(f_{parent} + f_{diluent})}, \quad (1)$$

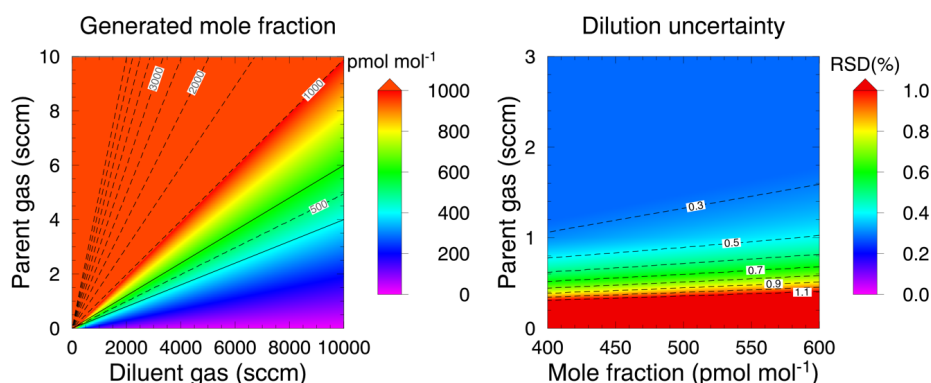
7
8 where $[x]$ indicates the mole fraction of gas x in the gas flow of the dynamically generated gas mixture
9 (*diluted*) and parent gas (*parent*) and f is the mass flow rate corresponding to the subscripted gas flow.
10 By applying the propagation law to this equation, the uncertainty in the mole fraction of the diluted gas
11 x can be estimated from the uncertainty of each variable associated with the gravimetric preparation and
12 Molbloc measurement as follows:

$$14 \quad u_{diluted} =$$
$$15 \quad \sqrt{\left\{ \frac{1}{(f_{parent} + f_{diluent})^2} \right\}^2 \cdot \left\{ (f_{parent}^2 \cdot \delta[x]_{parent}^2 \cdot (f_{parent} + f_{diluent})^2) + [x]_{parent}^2 \cdot (f_{diluent}^2 \cdot \delta f_{parent}^2 + f_{parent}^2 \cdot \delta f_{diluent}^2) \right\}^2}$$
$$16 \quad . \quad (2)$$

17
18 The dilution uncertainty associated only with the Molbloc measurements can be estimated by removing
19 the uncertainty derived from the gravimetric preparation of the parent gas ($\delta[x]_{parent} = 0$). The mole
20 fraction distributions of gas x and relevant dilution uncertainties are shown in Figure 2. The dilution
21 system can generate diluted gas mixtures across a wide range of mole fractions depending on the flow
22 rates of the diluent and parent gases, covering the typical mole fractions of COS in the atmosphere (400–
23 600 pmol mol⁻¹). The dilution uncertainty was determined using the flow rates and was found to change
24 significantly at flow rates corresponding to 10% full-scale for the Molbloc elements used. For example,
25 within the typical atmospheric COS mole fraction range, the uncertainty at parent gas flow rates below
26 1 sccm, which corresponds to a 10% full-scale flow rate, decreased rapidly from approximately 0.5%



1 with a decreasing flow rate. In contrast, the uncertainty remained nearly constant at parent gas flow rates
2 above 1 sccm. The parent gas flow rates above 2 sccm within the typical COS mole fraction range
3 suppressed the dilution uncertainty to below 0.3%.
4



5
6 **Figure 2: Mole fraction distribution for a dynamically diluted gas produced from a $1 \mu\text{mol mol}^{-1}$**
7 **parent gas mixture (left) and the corresponding dilution uncertainty (right). The two solid black**
8 **lines in the left panel indicate the typical mole fraction range of atmospheric COS ($400\text{--}600 \text{ pmol}$**
9 **mol^{-1}).**

10

11 **2.4 Determination of COS in a diluted gas mixture**

12 To evaluate dilution performance of our method, we measured the mole fractions of COS and HCFC-
13 22 (hereafter ‘target gases’) in dynamically diluted gas mixtures by using the sample determination
14 system. Because the details of the method used for target gas determination are presented in Saito et al.
15 (2010), only a general description is provided here. The gas mixture generated by the dilution system
16 was introduced via MFC-C into a dual-stage cryogenic preconcentration system at a constant flow rate
17 of 40 sccm for 12 min to enrich the target gases in the gas mixture. Concurrently with the enrichment,
18 the mass flow rates of the parent and diluent gases were recorded to calculate the mole fractions of the
19 target gases concentrated during the initial sample enrichment process. The cryogenically enriched
20 target gases were thermally desorbed, enriched again, and injected into the GC/MS for analysis. The



1 total measurement time for each sample was 1 h.

2 The target gas measurements were referenced against measurements of an ambient air-based
3 reference gas mixture to correct for diurnal variations in the sensitivity of the mass spectrometer. To
4 prepare the reference gas mixture, ambient air was dried to a dew-point temperature of less than $-80\text{ }^{\circ}\text{C}$
5 by passing it through a Nafion Perma Pure dryer (Perma Pure LLC; Toms River, NJ) and a chemical
6 trap packed with phosphorous pentoxide (Sicapent[®]; EMD Millipore, Billerica, MA) and subsequently
7 filled into a 48-L high-pressure aluminium cylinder with an inner surface that had been mirror polished
8 and anodised. Before filling, the aluminium cylinder was evacuated, and Milli-Q water was added so
9 that the water vapour mole fraction was approximately $500\text{ }\mu\text{mol mol}^{-1}$ at a maximum fill pressure of
10 14.7 MPa after gas filling to enhance the stability of the trace gases in the compressed air during storage
11 (Montzka et al., 2004; Hall et al., 2014).

12 The target gases in the reference gas mixture were measured before and after sample gas
13 measurement. The signal responses obtained from the GC/MS measurements were used to estimate the
14 change in GC/MS sensitivity during sample measurements by linear interpolation. The signals from the
15 sample measurements were normalised to the interpolated responses of the reference gas mixture and
16 then multiplied by the known mole fraction of the corresponding target gas in the reference gas mixture
17 as follows:

$$19 \quad [x]_{sample} = \frac{R_{x,sample}}{\hat{R}_{x,ref}} \times [x]_{ref}, \quad (3)$$

20

21 where the mole fractions of gas x in the sample and the reference gas mixture are indicated in square
22 brackets, and $R_{x,sample}$ and $\hat{R}_{x,ref}$ are the signal responses for gas x in the sample gas mixture and the
23 interpolated response for the reference gas mixture, respectively. The typical analytical precision for
24 COS and HCFC-22 was a relative standard deviation (RSD) of less than 0.5% during the study period.

25

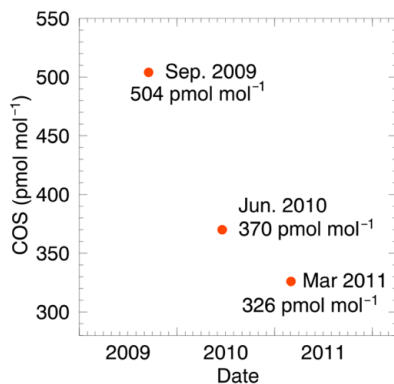
26 **3 Long-term stability of COS in high-pressure aluminium cylinders**



1 Atmospheric trace gases with dry mole fractions of sub-nanomole-per-mole levels such as COS and
2 halocarbons, can exhibit significant changes during storage in high-pressure cylinders. High-pressure
3 stainless steel cylinders are generally used for the storage of reference gas mixtures for these trace gases.
4 Previous studies have reported that COS and halocarbons show superior stability, even at ambient mole
5 fractions, in this type of cylinder (Hall et al., 2014; Guillevic et al., 2018). Thus, the use of stainless steel
6 cylinders can be an effective measure to reduce changes in the mole fractions of COS during storage.
7 However, in this study, we opted to use an aluminium cylinder because aluminium cylinders with treated
8 inner surfaces are easier for us to obtain than stainless steel cylinders.

9 In the past, we have prepared several COS reference gas mixtures at ambient levels filled in high-
10 pressure aluminium cylinders by the gravimetric method, and almost all of them showed substantial
11 changes in the mole fraction of COS during storage, which hereafter is referred to as ‘drift’. Figure 3
12 shows an example of drift, in which we observed an exponential decrease in the mole fraction of COS.
13 Although the stability during storage could be enhanced depending on the material of the gas cylinder
14 and inner-surface treatment (Yokohata et al., 1985; Montzka et al., 2004, 2007; Hall et al., 2014), other
15 factors that affect the amount and rate of this drift remain unknown. In contrast, we observed no notable
16 drift for gas mixtures containing COS at the micromole-per-mole level, suggesting that the amount of
17 drift is related to the amount of COS filled in the cylinder.

18 To examine this quantitatively, we determined the mole fraction of COS in compressed air filled in
19 a high-pressure manganese cylinder against three different COS reference gas mixtures containing
20 approximately $5 \mu\text{mol mol}^{-1}$ COS prepared in different years. The three COS reference gas mixtures
21 (balanced in nitrogen) were prepared gravimetrically and filled into 9.4-L aluminium cylinders at a fill
22 pressure of 9.81 MPa by a Japanese manufacturer (Japan Fine Products, Co.) in 2006, 2011, and 2015;
23 the nominal mole fractions of COS were 5.12, 5.02, and $5.05 \mu\text{mol mol}^{-1}$, respectively (Table 1). As
24 shown in this table, the COS mole fractions in compressed air determined by GC/MS can be compared
25 with one another for indirect evaluation of the long-term stability of COS at the micromole-per-mole
26 level in reference gas mixtures during storage.



1

2 **Figure 3: Time-series variation of the COS mole fraction in a reference gas mixture during long-**
3 **term storage in a high-pressure aluminium cylinder.**

4

5 To establish linearity of the GC/MS analysis for ambient-level COS, the gravimetric reference gas
6 mixtures were dynamically diluted 10,000 times with high-purity nitrogen to generate COS mole
7 fractions of approximately 500 pmol mol⁻¹. Gas dilution was performed using a commercially available
8 dynamic diluter (SGGU-7000NS-U6; HORIBA STEC, Co., Ltd.). We do not present the details of the
9 diluter here; only the general features are described. The diluter employed a two-step dilution method,
10 and the dilution was performed by mixing the parent and diluent gases at gas flow rates regulated by
11 two MFCs. The expected mole fraction from dilution was calculated from the measured flow rates of
12 the two gases. The nominal repeatability and precision of the dilutions were ± 0.5 and 1.0%, respectively.
13 The COS measurement was repeated four to eight times according to the protocol described in Section
14 2.4, until the measured values stabilised. The COS mole fraction was determined based on the final three
15 measurements.

16 The measurements of COS in the compressed air showed high repeatability, of which standard
17 deviations (1σ) were within 0.5 pmol mol⁻¹. The assigned COS values fell outside the 2-sigma range
18 but were within 2%. It is difficult to clarify whether a marked COS drift occurred in the reference gas
19 mixture owing to the unquantified combined uncertainty related to gravimetric preparation and dynamic
20 dilution. However, the results in Table 1 indicate no noticeable COS drift proportional to the storage



1 duration over a period of 10 years. These results imply that the impact of drift during storage is
2 practically negligible when using a gas mixture containing COS at a micromole-per-mole level. This
3 suggests an alternative approach to maintain the COS calibration scale with a high-accuracy dynamic
4 dilution of the quasi-stable reference gas mixture. Periodic absolute determination is still required for
5 stability validation; however, its frequency can be reduced significantly. We note that the COS
6 determination using the commercial dynamic dilutor in this experiment showed stable results from
7 several repeated measurements, but the measured values often remained unstable with less repeatability
8 and reproducibility. Thus, we need to develop a high-accuracy dynamic dilution method to prevent the
9 subjective assignment of unstable results, which could lead to significant bias.

10

11 **Table 1: Mole fractions of COS in compressed air determined by GC/MS calibrated against three**
12 **individual dynamically diluted gas mixtures prepared in different years.**

Reference gas mixture		COS assigned value (pmol mol^{-1}) [†]	
Preparation year	Nominal mole fraction ($\mu\text{mol mol}^{-1}$)	Average	Standard deviation (1σ)
2006	5.12	270.2	0.1
2011	5.02	274.6	0.4
2015	5.05	272.9	0.5

13 [†]COS determination was performed in March 2023.

14

15 **4 Evaluation of dilution performance**

16 We investigated the repeatability, reproducibility, and linearity of the developed dynamic dilution system.
17 We also examined the overall dilution accuracy based on the determination of HCFC-22. These
18 experiments were conducted based on GC/MS analysis of the target gases, and we report the GC/MS
19 measurements as response values normalised to an ambient air-based reference gas mixture according
20 to the procedure described in Section 2.4. After validating our dilution method, we assigned mole
21 fractions to the target gases in the ambient air-based reference gas mixture.



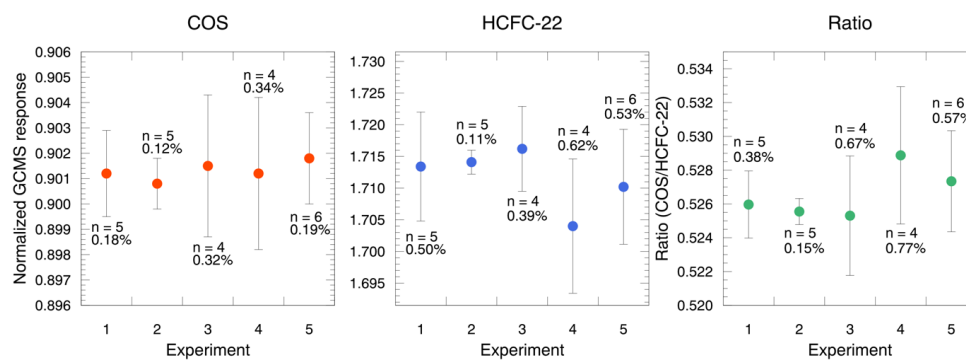
1

2 **4.1 Repeatability and reproducibility**

3 To evaluate repeatability and reproducibility, we conducted a series of experiments in which we
4 generated a diluted parent gas mixture using a dilution system, followed by GC/MS measurements of
5 the target gases. A total of five experiments were conducted, with each experiment consisting of at least
6 four sample measurements. Four of the experiments were performed on different days within a week,
7 and the final experiment was performed approximately two weeks after the previous four experiments.
8 A common dilution ratio was used in these experiments. The expected mole fraction of the diluted target
9 gases was approximately $500 \text{ pmol mol}^{-1}$ for COS and $495 \text{ pmol mol}^{-1}$ for HCFC-22, and the flow rates
10 of the parent and diluent gases to be blended were set at 2.5 and 5000 sccm, respectively. For each
11 experiment, the average and standard deviation of the response values from the GC/MS measurements
12 were calculated from at least four normalised responses.

13 Figure 4 shows the results of the GC/MS measurements of the diluted target gases. The RSD
14 values for the normalised responses of COS and HCFC-22 from each of the five experiments were
15 within 0.34% and 0.62%, respectively, and the average RSD values were 0.23% and 0.43%, respectively.
16 Although the RSD value was obtained as the combined uncertainty of the dynamic dilution and the
17 GC/MS measurements, the average RSD values were comparable to those of the typical measurement
18 repeatability of the GC/MS (0.5%). These results suggest that the repeatability obtained was primarily
19 subject to uncertainty from the GC/MS measurements rather than from the dilution process. On the other
20 hand, the normalised responses for both COS and HCFC-22 from the five experiments were in good
21 agreement. The RSD values for these responses were 0.04% for COS and 0.28% for HCFC-22,
22 indicating high reproducibility of the developed method. These excellent dilution performances were
23 corroborated by the ratio of the normalised response of COS to that of HCFC-22. We observed no clear
24 systematic changes in the normalised response ratios in each experiment and obtained nearly constant
25 average ratios among the five experiments. These results suggested that there was no significant dilution
26 bias in COS.

27



1

2 **Figure 4: Repeatability and reproducibility of our dynamic dilution method for generating gas**
3 **mixtures containing COS and HCFC-22. Vertical error bars indicate the standard deviation of the**
4 **normalized values obtained in each experiment. The number of measurements and relative**
5 **standard deviation are shown for each average plot.**

6

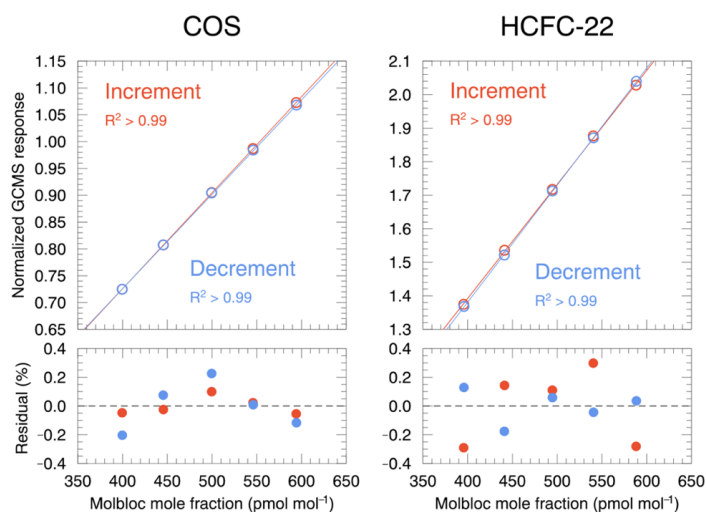
7 **4.2 Dilution linearity**

8 The dilution linearity was examined by comparing the measurements of the target gases in the generated
9 gas mixture determined by the Molbloc system with those obtained by the sample determination system
10 using GC/MS. The mole fractions of the target gases in the generated gas mixture were calculated from
11 the mass flow rates of the parent and diluent gases measured using the Molbloc system, whereas the
12 target gases were determined as normalised GC/MS responses based on GC/MS measurements. For the
13 experiment, the dilution ratio was varied by changing the parent gas flow rate using MFC-B such that
14 the expected mole fraction of COS in the generated gas mixture was in the range of 400–600 pmol mol⁻¹,
15 which corresponds to the typical atmospheric mole fraction. We checked the linear response of COS
16 and HCFC-22 in increments of 50 pmol mol⁻¹ in the range defined by the dilution ratio, and then we
17 checked in decrements of 50 pmol mol⁻¹ to investigate the possible memory effect of the previous
18 dilution process. The normalised GC/MS responses were plotted against the mole fractions obtained
19 from the Molbloc system (Figure 5). For the increment and decrement changes, the normalised COS
20 and HCFC-22 values showed excellent linearity with the corresponding mole fractions from the Molbloc



1 system, and linear least-squares fitting yielded determination coefficients greater than 0.99. The relative
2 residuals of the normalised values from the fitting line were also plotted (bottom panels). The values for
3 COS and HCFC-22 were distributed within 0.4%, which can be explained by the typical analytical
4 uncertainty (0.5%) of the sample determination GC/MS system. There was no clear dependence of the
5 relative residual values on the Molbloc mole fraction, and similar results were obtained for the ratio of
6 the normalised values (data not shown). These results indicated that there was no significant memory
7 effect from the previous blending process. Overall, our results demonstrate that our dynamic dilution
8 system has excellent linearity in the range of the investigated dilution ratios and shows no bias
9 depending on the mole fraction of the generated target gas.

10



11

12 **Figure 5: Dilution linearity of the dynamic dilution method for COS and HCFC-22 in response to**
13 **increases or decreases in the generated target gas mole fractions. The normalized GC/MS**
14 **responses (upper) and residuals from the fitting line determined by linear least squares (bottom)**
15 **are shown as a function of the mole fraction calculated from the average mass flow rates during**
16 **the sample concentration process measured by the Molbloc system.**

17

18 4.3 Validation of dilution accuracy



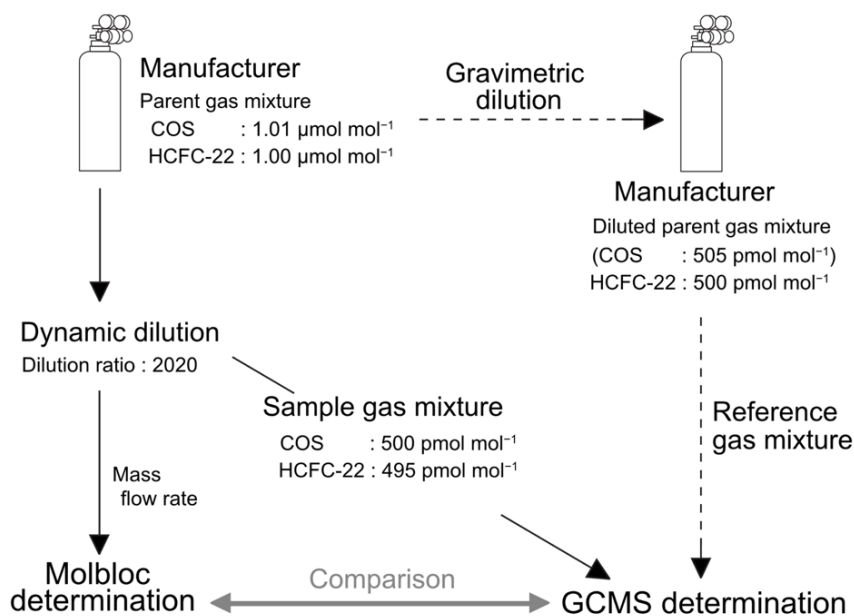
1 Next, the overall dilution accuracy of the dynamic dilution method was assessed using a validation
2 experiment. In the experiment, the mole fractions of the target gases in the dynamically diluted parent
3 gas mixture determined by the Molbloc system were compared with those determined by GC/MS
4 calibrated using a reference gas mixture (Figure 6). The reference gas mixture was prepared by the
5 Japanese gas manufacturer (Japan Fine Products, Co.) by gravimetric dilution of the parent gas mixture
6 with high-purity nitrogen and was filled in a 9.4-L high-pressure aluminium cylinder at a fill pressure
7 of 9.4 MPa. The nominal mole fractions of COS and HCFC-22 in the gas mixture were 505 and 500
8 pmol mol^{-1} , respectively. Owing to this gravimetric dilution, the GC/MS measurements were
9 standardised to those of the parent gas mixture. We expected a significant COS loss in the gravimetric
10 reference gas mixtures, and a marked decrease in COS was observed (reduced to approximately 1/13 of
11 the nominal value). However, we could analyse the dilution accuracy based on HCFC-22 determination
12 because our experiments demonstrated comparable dilution performances between HCFC-22 and COS.

13 In the experiment, the dynamically diluted parent gas mixture was generated by a 2020-fold
14 dilution to produce an expected HCFC-22 mole fraction of $495 \text{ pmol mol}^{-1}$. The generated gas mixture
15 was measured six times in series by GC/MS, and the average HCFC-22 mole fraction in the diluted gas
16 mixture during the preconcentration process of the GC/MS measurement was determined using the
17 Molbloc system, which measures the mass flow rates of the parent and diluent gases (Table 2).

18 We obtained average HCFC-22 values with high repeatability using both methods. The standard
19 deviations for the GC/MS and Molbloc measurements were 0.77 and $0.12 \text{ pmol mol}^{-1}$ and the
20 corresponding RSD values were 0.16 and 0.02% , respectively. There was a slight difference between
21 the two average values; the GC/MS measurements were approximately 2 pmol mol^{-1} lower than the
22 Molbloc measurements. The average values fell outside the 2-sigma range of one another, but the
23 observed difference was likely due to preparation uncertainty from the gravimetric dilution. Although
24 no estimated uncertainty was provided by the manufacturer, the observed difference corresponded to
25 0.4% of the nominal mole fraction of HCFC-22, which was acceptable as the gravimetric preparation
26 uncertainty. Based on these results, we concluded that there was no significant systematic bias due to
27 the dynamic dilution.



1



2

3 **Figure 6: Scheme for validating the dilution accuracy of our dynamic dilution method.**

4

5 **Table 2: Comparison of HCFC-22 mole fractions determined by GC/MS sample determination**
 6 **and Molbloc systems.**

Determination system	Method	Sample	HCFC-22 (pmol mol^{-1}) (n = 6)
Sample determination system	Preconcentration and GC/MS determination	Dynamically generated gas mixture	493.71 ± 0.77
Molbloc system	Mass flow rate measurements	Parent and diluent gases	495.77 ± 0.12
Difference (GC/MS – Molbloc)			-2.06 ± 0.78



1

2 **4.4 Mole fraction assignment of COS and HCFC-22 in a high-pressure aluminium cylinder**

3 Here, we present an example of mole fraction assignment for target gases in a high-pressure aluminium
4 cylinder using dynamic dilution and sample determination systems. By re-evaluating the experimental
5 data described in Section 4.1, we determined the mole fractions of COS and HCFC-22 in the ambient
6 air-based reference gas mixture, which was used to correct for diurnal variations in the sensitivity of
7 GC/MS. As described in Section 2.4, the mole fraction of gas x was expressed as the product of the
8 normalised GC/MS response and the assigned mole fraction of gas x in a reference gas mixture
9 according to equation (3). Rearranging equation (3) using the mole fraction determined from the
10 Molbloc measurements yields

11

$$12 \quad [x]_{ref} = \frac{\hat{R}_{x,ref}}{R_{x,diluted}} \times [x]_{diluted,Molbloc}, \quad (4)$$

13

14 where $R_{x,diluted}$ is the normalised GC/MS response for gas x in the dynamically diluted gas mixture and
15 $[x]_{diluted,Molbloc}$ is the average mole fraction calculated from the mass flow rates of the parent and diluent
16 gases measured by the Molbloc system during sample concentration. The assigned mole fraction values
17 for the target gases in the ambient air-based reference gas mixture are summarised in Table 3. The mole
18 fractions of COS and HCFC-22 were precisely determined because of the high repeatability and
19 reproducibility of the developed dynamic dilution method (see Section 4.1). The assigned values of COS
20 and HCFC-22 were 554.51 ± 0.13 and 289.11 ± 0.34 pmol mol⁻¹ and their corresponding relative
21 standard errors were 0.02% and 0.12%, respectively. These results were sufficiently accurate for the
22 determination of COS and HCFC-22 in gas mixtures. However, the values obtained were determined
23 against a gravimetrically prepared parent gas mixture. Therefore, absolute determination of the target
24 gases in the parent gas mixture is required to establish our COS calibration scale for atmospheric COS
25 observations.

26



1 **Table 3: Mole fraction assignment for the target gases in an ambient air-based reference gas**
2 **mixture based on the measurements by the Molbloc and sample determination systems.**

Experiment	COS		HCFC-22		Assigned mole fraction [†]	
	(pmol mol ⁻¹)		(pmol mol ⁻¹)		(pmol mol ⁻¹)	
	Mole fraction	Standard deviation	Mole fraction	Standard deviation	COS	HCFC-22
1	554.68	1.20	288.85	1.53		
2	554.65	1.03	288.61	0.53	554.51	289.11
3	554.72	2.01	288.51	1.02	± 0.13	± 0.34
4	554.52	1.87	290.37	1.81	(0.02%)	(0.12%)
5	554.00	1.23	289.25	1.48		

3 [†]Uncertainty is given as the standard error and the corresponding relative values are provided in
4 parentheses.

5

6 **5 Discussion**

7 We developed a dynamic dilution method for preparing reference gas mixtures containing COS that
8 includes a relative drift-reduction approach to avoid issues related to the change in the COS mole
9 fraction over time; however, outstanding issues still exist that may lead to reduced consumption of the
10 parent gas mixture in our dynamic dilution method.

11 In our pilot study, we found an unexplained dilution bias responsible for the inconsistent
12 determination of the target gases in the dynamically generated gas mixture between the GC/MS and
13 Molbloc measurements (see Supplemental Information). The dilution bias depended on the pressure and
14 flow rates of the parent and diluent gases; even under pressure control of the relevant gas flows, a greater
15 bias was observed for COS. We attributed this COS-specific dilution bias to factors possibly associated
16 with the adsorption of COS onto the inner surface of the dilution system or with gas fractionation
17 processes occurring at the cylinder and regulator during the passage of the parent gas flow through them.



1 Therefore, we improved our dilution method by increasing the system purge time, introducing a more
2 rigorous pressure matching between the two gas flows, and increasing the parent gas flow rate beyond
3 that required for generation of reference gas mixture, with excess flow exhausted via a branch exhaust
4 system. Consequently, the combination of these strategies worked well for high-accuracy dynamic
5 dilution in this study, although COS-specific bias is not clearly understood.

6 A similar dilution bias has been observed by Brewer et al. (2014). They reported that the
7 dynamically generated mole fractions of SO₂ and CO showed a systematic bias that was inversely
8 proportional to the parent gas flow rate at flow rates of less than 10 mL/min. In our experiments, the
9 dilution accuracy deteriorated at these flow rates before improvements were made to the system;
10 however, no clear inverse dependence was observed, implying that the dilution bias was not limited to
11 COS dilution, and its impact and biasing can vary in a complicated manner, probably depending on the
12 experimental conditions and physical properties of the diluted gases, especially at a lower flow rate of
13 the parent gas. On the other hands, previous studies identified several factors that can cause gas
14 fractionation in gases flowing from a high-pressure cylinder via a pressure regulator. Gas fractionation
15 can be caused by kinetic processes owing to diffusive fractionation, such as pressure diffusion, thermal
16 diffusion, effusion, and gas adsorption to the inner wall of the cylinder (Langenfelds et al., 2005; Schibig
17 et al., 2018; Hall et al., 2019; Aoki et al., 2022). Given that we previously suggested the possible
18 involvement of the cylinder and regulator, these diffusive processes may contribute to the observed
19 dilution bias, with a strong influence on COS dilution. Further investigations are required to identify the
20 mechanisms underlying the observed dilution bias.

21 It is important to note that the precision of the developed dynamic dilution method is inferior to
22 that of gravimetry at this stage; however, the developed method has a practical advantage for
23 atmospheric COS observation because of the limited storage stability of COS in high-pressure cylinders.
24 A further advantage is that the new technical knowledge obtained from this study will allow us to
25 establish a fully automated dynamic dilution system. This will expand the application of the dilution
26 system by reducing the labour and time required to conduct experiments. For example, the international
27 WMO Global Atmosphere Watch program has set a goal of $\pm 2 \text{ nmol mol}^{-1}$ for inter-laboratory



1 compatibility for atmospheric CO measurements (WMO, 2020). In high-pressure aluminium cylinders,
2 CO is generally known to show substantial positive growth (Novelli et al., 1994, 2003; Tanimoto et al.,
3 2007; Nara et al., 2011), but the impact of CO growth can be relatively reduced at the micromolar-per-
4 mole level (Nara et al., 2011), suggesting that our relative drift-reduction approach will most likely
5 maintain the quasi-integrity of CO in the reference gas mixtures at higher CO mole fractions. Because
6 the dilution accuracy of our developed method was estimated to be within 0.1% RSD for the mole
7 fraction of the generated gas, our dynamic dilution approach can contribute greatly to fulfilling the
8 WMO compatibility goal, even without gravimetric preparation. This emphasises the usefulness of our
9 dynamic dilution method with a relative drift-reduction approach for maintaining the reference gas scale
10 and traceability of unstable trace gases at ambient levels.

11

12 **Summary and conclusion**

13 We developed a one-step dynamic dilution method that is capable of accurately generating COS
14 reference gas mixtures at ambient levels (ca. 500 pmol mol⁻¹) from a gravimetrically prepared parent
15 gas mixture containing a high mole fraction of COS (micromole-per-mole level).

16 We began by investigating the stability of ambient levels of COS stored in a high-pressure
17 aluminium cylinder. Although an exponential decrease in the mole fraction of COS was observed over
18 time, at higher mole fractions (approximately 5 μmol mol⁻¹), COS gravimetric gas mixtures were
19 practically stable for at least for 10 years. These results suggested that the impact of COS drift during
20 storage can be reduced to a negligible level using a gas mixture containing a high mole fraction of COS.
21 By applying this drift-reduction approach, we established a dynamic dilution method that uses a
22 gravimetric parent gas mixture containing approximately 1 μmol mol⁻¹ of COS, together with HCFC-
23 22, which was added to aid in diagnosing the cause of the dilution bias of COS observed in our pilot
24 study.

25 In the pilot study, the GC/MS response ratio of COS to HCFC-22 revealed an unexplained marked
26 bias for the dilution of the gravimetric parent gas mixture, with a greater bias for COS than for HCFC-
27 22. Although we could not identify the reason for this COS-specific dilution bias, it was considerably



1 improved by implementing strategies against the possible dilution-biasing factors of adsorption and gas
2 fractionation at the cylinder and regulator. The addition of a branch exhaust system was part of this
3 strategy, which helped rinse the flow path in the dilution system and stabilise the flow pressure of the
4 gravimetric parent gas while exhausting the excess parent gas flow. After implementing these
5 improvements, excellent repeatability and reproducibility were obtained for the dilution of COS and
6 HCFC-22 and for dilution linearity in our evaluation experiments. RSD values of 0.23% and 0.04% for
7 COS and 0.43% and 0.28% for HCFC-22 were obtained for the repeatability and reproducibility of the
8 method. This excellent dilution performance was corroborated by the nearly constant ratio of the
9 normalised GC/MS response of COS to that of HCFC-22. We obtained a comparable dilution
10 performance between COS and HCFC-22, allowing us to validate the dilution accuracy at ambient levels
11 for HCFC-22 by comparing the flow rate-based determination using the Molbloc system and GC/MS-
12 based determination system using a gravimetrically diluted parent gas mixture. A good agreement was
13 obtained between the two methods, demonstrating that our dynamic dilution method can accurately
14 generate diluted gas mixtures without significant systematic bias. Finally, we determined the mole
15 fractions of COS and HCFC-22 in an ambient air-based reference gas mixture by reevaluating the
16 experimental data obtained by testing the repeatability and reproducibility of the dilution method. The
17 mole fractions of COS and HCFC-22 were precisely determined, with relative standard errors of 0.02%
18 and 0.12%, respectively.

19 Overall, these results demonstrated that our dynamic dilution method can contribute to accurate
20 long-term observations of atmospheric COS. However, the absolute determination of COS in a
21 gravimetric parent gas mixture is needed to ensure traceability and interlaboratory compatibility; thus,
22 further development is needed to better understand atmospheric COS dynamics. Notably, our dilution
23 method can be applied to the preparation of other reference gas mixtures containing unstable
24 atmospheric trace gases such as CO in high-pressure cylinders, which emphasises the usefulness of our
25 dynamic dilution method.

26



1 **Author contributions**

2 HN performed conceptualization, funding acquisition, investigation, methodology. TS, TU, and YT
3 contributed to methodology and resources. HN drafted the paper with inputs from TS, TU, and YT. All
4 authors contributed to the discussion and improvement of the paper.

5

6 **Competing Interests**

7 The authors declare that they have no known competing financial interests or personal relationships that
8 could have appeared to influence the work reported in this paper.

9

10 **Acknowledgement**

11 The authors wish to thank K. Ooyama for his valuable comments on the pressure regulation of gas flow
12 from a high-pressure cylinder. We also thank N. Aoki for his valuable comments and technical support
13 in the gravimetric preparation of COS standard gas. This work was funded mainly by a research and
14 development project from the National Institute for Environmental Studies and partially by the Air
15 Quality and Climate Change Program of the National Institute for Environmental Studies and a Grant-
16 in-Aid for Scientific Research (S) [22H05006].

17

18 **References**

19 Aoki, N., Ishidoya, S., Murayama, S., and Matsumoto, N.: Influence of CO₂ adsorption on cylinders and
20 fractionation of CO₂ and air during the preparation of a standard mixture, *Atmos. Meas. Tech.*, 15,
21 5969–5983. <https://doi.org/10.5194/amt-15-5969-2022>, 2022.

22 Asaf, D., Rotenberg, E., Tatarinov, F., Dicken, U., Montzka, S.A., and Yakir, D.: Ecosystem
23 photosynthesis inferred from measurements of carbonyl sulphide flux, *Nat. Geosci.*, 6, 186–190.
24 <https://doi.org/10.1038/NGEO1730>, 2013.

25 Blonquist Jr., J.M., Montzka, S.A., Munger, J.W., Yakir, D., Desai, A.R., Dragoni, D., Griffis, T.J.,
26 Monson, R.K., Scott, R.L., and Bowling, D.R.: The potential of carbonyl sulfide as a proxy for



- 1 gross primary production at flux tower sites, *J. Geophys. Res.*, 116, G04019.
2 <https://doi.org/10.1029/2011JG001723>, 2011.
- 3 Brewer, P.J., Goody, B.A., Woods, P.T., and Milton, M.J.T.: A dynamic gravimetric standard for trace
4 water, *Rev. Sci. Inst.*, 82, 105102. <https://doi.org/10.1063/1.3642660>, 2011.
- 5 Brewer, P.J., Miñarro, M.D., Di Meane, E.A., and Brown, R.J.C.: A high accuracy dilution system for
6 generating low concentration reference standards of reactive gases, *Measurement*, 47, 607–612.
7 <https://doi.org/10.1016/j.measurement.2013.09.045>, 2014.
- 8 Brühl, C., Lelieveld, J., Crutzen, P.J., and Tost, H.: The role of carbonyl sulphide as a source of
9 stratospheric sulphate aerosol and its impact on climate, *Atmos. Chem. Phys.*, 12, 1239–1253.
10 <https://doi.org/10.5194/acp-12-1239-2012>, 2012.
- 11 Campbell, J.E., Berry, J.A., Seibt, U., Smith, S.J., Montzka, S.A., Launois, T., Belviso, S., Bopp, L., and
12 Laine, M.: Large historical growth in global terrestrial gross primary production, *Nature*, 544, 84–
13 87. <https://doi.org/10.1038/nature22030>, 2017.
- 14 Campbell, J.E., Carmichael, G.R., Chai, T., Mena-Carrasco, M., Tang, Y., Blake, D.R., Blake, N.J., Vay,
15 S.A., Collatz, G.J., Baker, I., Berry, J.A., Montzka, S.A., Sweeney, C., Schnoor, J.L., and Stanier,
16 C.O.: Photosynthetic control of atmospheric carbonyl sulfide during the growing season, *Science*,
17 322, 1085–1088. <https://doi.org/10.1126/science.1164015>, 2008.
- 18 Chin, M. and Davis, D.D.: A reanalysis of carbonyl sulfide as a source of stratospheric background
19 sulfur aerosol, *J. Geophys. Res.*, 100, 8993–9005. <https://doi.org/10.1029/95JD00275>, 1995.
- 20 Commane, R., Herndon, S.C., Zahniser, M.S., Lerner, B.M., McManus, J.B., Munger, J.W., Nelson,
21 D.D., and Wofsy, S.C.: Carbonyl sulfide in the planetary boundary layer: Coastal and continental
22 influences, *J. Geophys. Res.*, 118, 8001–8009. <https://doi.org/10.1002/jgrd.50581>, 2013.
- 23 Flores, E., Viallon, J., Moussay, P., Idrees, F., and Wielgosz, R.I.: Highly accurate nitrogen dioxide
24 (NO_2) in nitrogen standards based on permeation, *Anal. Chem.*, 84, 10283–10290.
25 <https://doi.org/10.1021/ac3024153>, 2012.
- 26 Fried, A., Nunnermacker, L., Cadoff, B., Sams, R., Yates, N., Dorko, W., Dickerson, R., and Winstead,
27 E.: Reference NO_2 calibration system for ground-based intercomparisons during NASA's



- 1 GTE/CITE 2 Mission, J. Geophys. Res., 95, 10139–10146.
2 <https://doi.org/10.1029/JD095iD07p10139>, 1990.
- 3 Goldan, P.D., Fall, R., Kuster, W., and Fehsenfeld, F.C.: Uptake of COS by growing vegetation: a major
4 tropospheric sink, J. Geophys. Res., 93, 14186–14192. <https://doi.org/10.1029/JD093iD11p1418>,
5 1988.
- 6 Goldan, P.D. and Kuster, W.C.: A dynamic dilution system for the production of sub-ppb concentrations
7 of reactive and labile species, Atmos. Environ., 20, 1203–1209. <https://doi.org/10.1016/0004->
8 [6981\(86\)90154-X](https://doi.org/10.1016/0004-6981(86)90154-X), 1986.
- 9 Goody, B.A. and Milton, M.J.T.: High-accuracy gas flow dilutor using mass flow controllers with binary
10 weighted flows, Meas. Sci. Technol., 13, 1138–1145. <https://doi.org/10.1088/0957-0233/13/7/323>,
11 2002.
- 12 Guillevic, M., Vollmer, M.K., Wyss, S.A., Leuenberger, D., Ackermann, A., Pascale, C., Niederhauser,
13 and B., and Reimann, S.: Dynamic–gravimetric preparation of metrologically traceable primary
14 calibration standards for halogenated greenhouse gases, Atmos. Meas. Tech., 11, 3351–3372.
15 <https://doi.org/10.5194/amt-11-3351-2018>, 2018.
- 16 Hall, B.D., Engel, A., Mühle, J., Elkins, J.W., Artuso, F., Atlas, E., Aydin, M., Blake, D., Brunke, E.-G.,
17 Chiavarini, S., Fraser, P.J., Happell, J., Krummel, P.B., Levin, I., Loewenstein, M., Maione, M.,
18 Montzka, S.A., O’Doherty, S., Reimann, S., Rhoderick, G., Saltzman, E.S., Scheel, H.E., Steele,
19 L.P., Vollmer, M.K., Weiss, R.F., Worthy, D., and Yokouchi, Y.: Results from the International
20 Halocarbons in Air Comparison Experiment (IHALACE), Atmos. Meas. Tech., 7, 469–490.
21 <https://doi.org/10.5194/amt-7-469-2014>, 2014.
- 22 Hall, B.D., Crotwell, A.M., Miller, B.R., Schibig, M., and Elkins, J.W.: Gravimetrically prepared carbon
23 dioxide standards in support of atmospheric research, Atmos. Meas. Tech., 12, 517–524,
24 <https://doi.org/10.5194/amt-12-517-2019>, 2019.
- 25 ISO 6142-1: Gas analysis–Preparation of calibration gas mixtures–Part 1: Gravimetric method for Class
26 I mixtures, available at: <https://www.iso.org/standard/59631.html> (last access: Jan 2023), 2015.
- 27 ISO 6145-7: Gas analysis–Preparation of calibration gas mixtures using dynamic methods–Part 7:



- 1 Thermal mass-flow, available at: <https://www.iso.org/standard/45471.html> (last access: Jan 2023),
2 2018.
- 3 Kerwin, R.A., Crill, P.M., Talbot, R.W., Hines, M.E., Shorter, J.H., Kolb, C.E., and Harriss, R.C.:
4 Determination of atmospheric methyl bromide by cryotrapping-gas chromatography and
5 application to soil kinetic studies using a dynamic dilution system, *Anal. Chem.*, 68, 899–903.
6 <https://doi.org/10.1021/ac950811z>, 1996.
- 7 Kim, M.E., Kim, Y.D., Kang, J.H., Heo, G.S., Lee, D.S., and Lee, S.: Development of traceable precision
8 dynamic dilution method to generate dimethyl sulphide gas mixtures at sub-nanomole per mole
9 levels for ambient measurement, *Talanta*, 150, 516–524.
10 <https://doi.org/10.1016/j.talanta.2015.12.063>, 2016.
- 11 Kjellstrom, E.: A three-dimensional global model study of carbonyl sulfide troposphere and the lower
12 stratosphere, *J. Atmos. Chem.*, 29, 151–177. <https://doi.org/10.1023/A:1005976511096>, 1998.
- 13 Kooijmans, L.M.J., Sun, W., Aalto, J., Erkkilä, K., Maseyk, K., Seibt, U., Vesala, T., Mammarella, I.,
14 and Chen, H.: Influences of light and humidity on carbonyl sulfide-based estimates of
15 photosynthesis, *P. Natl. Acad. Sci. USA*, 116, 2470–2475.
16 <https://doi.org/10.1073/pnas.1807600116>, 2019.
- 17 Landau, L. and Lifshitz, E.: Fluid mechanics 2nd edition, Course of theoretical Physics, Volume 6, 1987.
- 18 Langenfelds, R.L., van der Schoot, M.V., Francey, R.J., Steele, L.P., Schmidt, M., and Mukai, H.:
19 Modification of air standard composition by diffusive and surface processes, *J. Geophys. Res.*,
20 110, D13307. <https://doi.org/10.1029/2004JD005482>, 2005.
- 21 Macé, T., Iturrate-Garcia, M., Pascale, C., Niederhauser, B., Vaslin-Reimann, S., and Sutour, C.: Air
22 pollution monitoring: development of ammonia (NH₃) dynamic reference gas mixtures at
23 nanomoles per mole levels to improve the lack of traceability of measurements, *Atmos. Meas.*
24 *Tech.*, 15, 2703–2718. <https://doi.org/10.5194/amt-15-2703-2022>, 2022.
- 25 Maseyk, K., Berry, J.A., Billesbach, D., Campbell, J.E., Torn, M.S., Zahniser, M., and Seibt, U.: Sources
26 and sinks of carbonyl sulfide in an agricultural field in the Southern Great Plains, *P. Natl. Acad.*
27 *Sci. USA*, 111, 9064–9069. <https://doi.org/10.1073/pnas.1319132111>, 2014.



- 1 Mohamad, G.H.P., Coles, G.S.V., and Watson, J.: An automatic low-level gas blender, *Trans. Inst. Meas.*
2 *Cont.*, 18, 62–68. <https://doi.org/10.1177/0142331296018002>, 1996.
- 3 Montzka, S., Aydin, M., Battle, M., Butler, J., Saltzman, E., Hall, B., Clarke, A., Mondeel, D., and Elkins,
4 J.: A 350-year atmospheric history for carbonyl sulfide inferred from Antarctic firn air and air
5 trapped in ice, *J. Geophys. Res.*, 109, D22302. <https://doi.org/10.1029/2004JD004686>, 2004.
- 6 Montzka, S.A., Calvert, P., Hall, B.D., Elkins, J.W., Conway, T.J., Tans, P.P., and Sweeney, C.: On the
7 global distribution, seasonality, and budget of atmospheric carbonyl sulfide (COS) and some
8 similarities to CO₂, *J. Geophys. Res. Atmos.*, 112, D09302.
9 <https://doi.org/10.1029/2006JD007665>, 2007.
- 10 Nakao, S. and Takamoto, M.: Development of the calibration facility for small mass flow rates of gases
11 and the sonic venturi nozzle transfer standard, *JSME Int. J. Ser. B.*, 42, 667–673.
12 <https://doi.org/10.1299/jsmeb.42.667>, 1999.
- 13 Nara, H., Tanimoto, H., Nojiri, H., Mukai, H., Machida, T., and Tohjima, Y.: Onboard measurement
14 system of atmospheric carbon monoxide in the Pacific by voluntary observing ships, *Atmos. Meas.*
15 *Tech.*, 4, 2495–2507. <https://doi.org/10.5194/amt-4-2495-2011>, 2011.
- 16 Nara, H., Tanimoto, H., Tohjima, Y., Mukai, H., Nojiri, Y., Katsumata, K., and Rella, C.W.: Effect of air
17 composition (N₂, O₂, Ar, and H₂O) on CO₂ and CH₄ measurement by wavelength-scanned cavity
18 ring-down spectroscopy: calibration and measurement strategy, *Atmos. Meas. Tech.*, 5, 2689–
19 2701. <https://doi.org/10.5194/amt-5-2689-2012>, 2012.
- 20 Novelli, P.C., Collins Jr., J.E., Myers, R.C., Sachse, G.W., and Scheel, H.E.: Reevaluation of the
21 NOAA/CMDL carbon monoxide reference scale and comparison with CO reference gases at
22 NASA-Langley and Fraunhofer Institute, *J. Geophys. Res.*, 99, 12833–12839.
23 <https://doi.org/10.1029/94JD00314>, 1994.
- 24 Novelli, P.C., Masarie, K.A., Lang, P.M., Hall, B.D., Myers, R.C., and Elkins, J.W.: Reanalysis of
25 tropospheric CO trends: effects of the 1997–1998 wildfires, *J. Geophys. Res.*, 108, 4464.
26 <https://doi.org/10.1029/2002JD003031>, 2003.



- 1 Protoschill-Krebs, G., Wilhelm, C., and Kesselmeier, J.: Consumption of carbonyl sulphide (COS) by
2 higher plant carbonic anhydrase (CA), *Atmos. Environ.*, 30, 3151–3156.
3 [https://doi.org/10.1016/1352-2310\(96\)00026-X](https://doi.org/10.1016/1352-2310(96)00026-X), 1996.
- 4 Saito, T., Yokouchi, Y., Stohl, A., Taguchi, S., and Mukai, H: Large emissions of perfluorocarbons in
5 East Asia deduced from continuous atmospheric measurements, *Environ. Sci. Technol.*, 44, 4089–
6 4095. <https://doi.org/10.1021/es1001488>, 2010.
- 7 Sandoval-Soto, L., Stanimirov, M., von Hobe, M., Schmitt, V., Valdes, J., Wild, A., and Kesselmeier, J.:
8 Global uptake of carbonyl sulfide (COS) by terrestrial vegetation: Estimates corrected by
9 deposition velocities normalized to the uptake of carbon dioxide (CO₂), *Biogeosciences*, 2, 125–
10 132. <https://doi.org/10.5194/bg-2-125-2005>, 2005.
- 11 Schibig, M.F., Kitzis, D., and Tans, P.P.: Experiments with CO₂-in-air reference gases in high-pressure
12 aluminum cylinders, *Atmos. Meas. Tech.*, 11, 5565–5586. [https://doi.org/10.5194/amt-11-5565-](https://doi.org/10.5194/amt-11-5565-2018)
13 [2018](https://doi.org/10.5194/amt-11-5565-2018), 2018.
- 14 Seibt, U., Kesselmeier, J., Sandoval-Soto, L., Kuhn, U., and Berry, J.A.: A kinetic analysis of leaf uptake
15 of COS and its relation to transpiration, photosynthesis and carbon isotope fractionation,
16 *Biogeosciences*, 7, 333–341. <https://doi.org/10.5194/bg-7-333-2010>, 2010.
- 17 Stimler, K., Berry, J.A., and Yakir, D.: Effects of carbonyl sulfide and carbonic anhydrase on stomatal
18 conductance^{1,[OA]}, *Plant Physiol.*, 158, 524–530. <https://doi.org/10.1104/pp.111.185926>, 2012.
- 19 Stimler, K., Montzka, S.A., Berry, J.A., Rudich, Y., and Yakir, D.: Relationships between carbonyl
20 sulfide (COS) and CO₂ during leaf gas exchange, *New Phytol.*, 186, 869–878.
21 <https://doi.org/10.1111/j.1469-8137.2010.03218.x>, 2010.
- 22 Tanimoto, H., Sawa, Y., Matsueda, H., Yonemura, S., Wada, A., Mukai, H., Wang, T., Poon, S., Wong,
23 A., Lee, G., Jung, J.Y., Kim, K.R., Lee, M., Lin, N.H., Wang, J.L., Ou-Yang, C.F., and Wu, C.F.:
24 Evaluation of standards and methods for continuous measurements of carbon monoxide at ground-
25 based sites in Asia, *Pap. Meteorol. Geophys.*, 58, 85–93. <https://doi.org/10.2467/mripapers.58.85>,
26 2007.



- 1 Tera Term project team, Tera Term 4.97 (Version 4.97), November 30, 2017.
2 <https://tssh2.osdn.jp/index.html.en>. (last access: Jan 2023).
- 3 Wehr, R., Munger, J.W., McManus, J.B., Nelson, D.D., Zahniser, M.S., Davidson, E.A., Wofsy, S.C.,
4 and Saleska, S.R.: Seasonality of temperate forest photosynthesis and daytime respiration, *Nature*,
5 534, 680–683. <https://doi.org/10.1038/nature17966>, 2016.
- 6 WMO: Scientific assessment of ozone depletion, 2018, GAW Report 58, World Meteorological
7 Organization (WMO), Global Ozone Research and Monitoring Project, Geneva, Switzerland,
8 available at: [https://public-old.wmo.int/en/resources/library/scientific-assessment-of-ozone-](https://public-old.wmo.int/en/resources/library/scientific-assessment-of-ozone-depletion-2018)
9 [depletion-2018](https://public-old.wmo.int/en/resources/library/scientific-assessment-of-ozone-depletion-2018) (last access: Jan 2023), 2018.
- 10 WMO: Scientific assessment of ozone depletion, 2022, GAW Report 278, World Meteorological
11 Organization (WMO), Global Ozone Research and Monitoring Project, Geneva, Switzerland,
12 available at: <https://www.csl.noaa.gov/assessments/ozone/2022/> (last access: Oct 2023), 2022.
- 13 WMO: Report of the 20th WMO/IAEA Meeting on carbon dioxide, other greenhouse gases and related
14 measurement techniques, 2–5 September 2019, GAW Report No. 255, available at:
15 https://library.wmo.int/index.php?lvl=notice_display&id=21758 (last access: Jan 2023), 2020.
- 16 Wright, R.S. and Murdoch, R.W.: Laboratory evaluation of gas dilution systems for analyser calibration
17 and calibration gas analysis, *Air Waste*, 44, 428–430.
18 <https://doi.org/10.1080/1073161X.1994.10467265>, 1994.
- 19 Yang, F., Qubaja, R., Tatarinov, F., Rotenberg, E., and Yakir, D.: Assessing canopy performance using
20 carbonyl sulfide measurements, *Glob. Chang. Biol.*, 24, 3486–3498.
21 <https://doi.org/10.1111/gcb.14145>, 2018.
- 22 Yokohata, A., Makide, Y., and Tominaga, T.: A new calibration method for the measurement of CCl₄
23 concentration at 10⁻¹⁰ v/v level and the behavior of CCl₄ in the atmosphere, *B. Chem. Soc. Jpn.*,
24 58, 1308–1314. <https://doi.org/10.1246/bcsj.58.1308>, 1985.